IL NUOVO CIMENTO Vol. 33 C, N. 2 Marzo-Aprile 2010
DOI 10.1393/ncc/i2010-10605-2

Colloquia: LC09

Higgs sector of the MSSM: Lepton flavor violation at colliders and neutralino dark matter

M. Cannoni([1]) and O. Panella([2])

([1]) *Departamento de Fisica Aplicada, Universidad de Huelva - Campus de El Carmen 21071 Huelva, Spain*
([2]) *INFN, Sezione di Perugia - Via A. Pascoli, 06129 Perugia, Italy*

(ricevuto il 18 Febbraio 2010; approvato il 25 Marzo 2010; pubblicato online il 18 Giugno 2010)

Summary. — We examine the prospects for the detection of Higgs-mediated lepton flavor violation at LHC and at a photon collider in the minimal supersymmetric standard model with large lepton flavor violating mass insertions in the $\mu - \tau$ sector constraining the parameter space with several experimental bounds. We find rates probably too small to be observed at future experiments if models have to accommodate for a neutralino relic density as measured by WMAP and explain the $(g-2)_\mu$ anomaly: better prospects are found if these two constraints are applied only as upper bounds. The spin-independent neutralino-nucleon cross-section in the studied constrained parameter space is just below the present CDMS limit while gamma rates from neutralino annihilation in the halo are strongly suppressed.

PACS 11.30.Pb – Supersymmetry.
PACS 14.80.Da – Supersymmetric Higgs bosons.
PACS 95.35.+d – Dark matter (stellar, interstellar, galactic, and cosmological).

1. – Introduction

The Higgs sector of the minimal supersymmetric standard model (MSSM) [1], especially the heavy neutral Higgses A and H, play a prominent role in the physics of neutralino dark matter [2]. In some region of the supersymmetric (SUSY) parameter space neutralinos yield the desired amount of relic density by annihilating into fermions through the s-channel resonant exchange of neutral Higgs bosons h, H, A, the so-called funnel region where $m_A \simeq 2m_\chi$; besides, as dark matter is expected to be distributed in a halo surrounding our galaxy, neutralinos can scatter off nuclei in terrestrial detectors: the coherent scattering is mediated by scalar interactions through the s-channel exchange of squarks and t-channel exchange of the CP-even neutral Higgs bosons h and H. These effects become sizable when squarks are heavy and $\tan\beta$ is large in reason of the enhanced Higgs bosons coupling to down-type fermions, especially for the b quark

which has the largest Yukawa coupling receiving large radiative SUSY-QCD corrections at large $\tan\beta$.

Once a source of lepton flavor violation (LFV) is present in the slepton mass matrix, for example the MSSM with the seesaw mechanism for generation of small neutrino masses [3], non-holomorphic LFV Yukawa couplings of the type $\bar{L}^i_R L^j_L H^*_u$ are induced at loop level and become particularly sizable at large $\tan\beta$ giving rise to enhanced Higgs-mediated LFV effects [4]. The LFV mass insertions $\delta^{ij}_{LL} = (m^2_L)^{ij}/m^2_L$, $\delta^{ij}_{RR} = (m^2_R)^{ij}/m^2_R$, where $(m^2_{L,R})^{ij}$ are the off-diagonal flavor changing entries of the slepton mass matrix, are free parameters which allow for a model-independent study of LFV signals. We introduce LFV in the model through the mass insertions $\delta^{32}_{LL,RR} = 0.5$. This value ensures the largest rates in LFV processes and allows us to study the more optimistic scenarios for LFV detection; higher values contradict the mass insertion approximation as an expansion of propagators in these small parameters.

Higgs-mediated effects become interesting at large μ and $\tan\beta$ and low m_A; further, if SUSY-QCD particles are heavy, Higgs effects are dominant also for neutralino dark matter. We thus consider the following real MSSM parameter space: $100\,\text{GeV} \leq m_A \leq 1\,\text{TeV}$, $20 \leq \tan\beta \leq 60$, $500\,\text{GeV} \leq \mu \leq 5\,\text{TeV}$, (the sign of μ is taken positive, as preferred by the SUSY explanation of the $(g-2)_\mu$ anomaly), $150\,\text{GeV} \leq M_1$, $M_2 \leq 1.5\,\text{TeV}$ (we do not impose any relation but let them vary independently allowing for gaugino non-universality at the weak scale), $1\,\text{TeV} \leq M_3 \leq 5\,\text{TeV}$ (to have large masses for gluinos), $1\,\text{TeV} \leq m_{U_3}, m_{D_3}, m_{Q_3} \leq 5\,\text{TeV}$ (for the first and the second generation the soft masses are set to be equal, $m_{U_i} = m_{D_i} = m_{Q_i} = m_{\tilde{q}}$, where $i = 1, 2$ and $m_{\tilde{q}}$ is another free parameter which varies in the same range), $300\,\text{GeV} \leq m_{L_3}, m_{E_3} \leq 2.5\,\text{TeV}$ (for the first and the second generation the slepton soft masses are set to be equal, $m_{L_i} = m_{E_i} = m_{\tilde{\ell}}$, where $i = 1, 2$ and $m_{\tilde{\ell}}$), $-2 \leq \frac{A_{U_3}}{m_{U_3}}, \frac{A_{D_3}}{m_{D_3}}, \frac{A_{E_3}}{m_{E_3}} \leq 2$ while for the first and the second generation the trilinear scalar couplings are set to zero.

We impose on the parameter space several experimental limits: 1) LEP, TEVATRON bounds on sparticle masses and the LEP bound on light Higgs; 2) present bounds on B-physics observables $\mathcal{B}(B \to X_s\gamma)$, $\mathcal{B}(B_s \to \mu^+\mu^-)$, Δm_{B_s}, $\mathcal{B}(B \to \tau\nu)$; 3) the present experimental upper bounds on LFV processes $\mathcal{B}(\tau \to \mu\gamma)$, $\mathcal{B}(\tau \to \mu\eta)$, $\mathcal{B}(\tau \to \mu\mu\mu)$, 4) the exclusion limits on the neutralino-nucleus spin-independent cross-section from the CDMS experiment [5]; 5) the CDF exclusion limits in the $(m_A, \tan\beta)$-plane [6]. All of them are applied at the same time with the exception of the WMAP 3σ interval [7] on relic density and $(g-2)_\mu$ anomaly for which we also relax the lower bounds: thus in the following figures the light gray (turquoise) points have only $\Omega_\chi h^2 \leq 0.13$ and $a^{\text{MSSM}}_\mu \leq 4 \times 10^{-9}$, the plus-shaped points dark-gray (indigo) points satisfies $0.09 \leq \Omega_\chi h^2 \leq 0.13$ and $a^{\text{MSSM}}_\mu \leq 4 \times 10^{-9}$, finally, the squared points satisfy $0.09 \leq \Omega_\chi h^2 \leq 0.13$ and $1\times10^{-9} \leq a^{\text{MSSM}}_\mu \leq 4\times10^{-9}$. For numerical computations we use the code DarkSusy [8] and the code FeynHiggs [9], while for the explicit formulas and further details on the experimental constraints we refer the reader to ref. [10].

2. – Higgs-mediated LFV at LHC and at a photon collider

At high $\tan\beta$ the dominant production mechanisms for A, H at LHC is $b\bar{b}$ fusion due to the $m_b \tan\beta$ enhanced $b\bar{b}\Phi$ couplings. We calculate the cross-section with FeynHiggs which uses the approximation $\sigma^{\text{MSSM}}(b\bar{b} \to \Phi) = \sigma^{\text{SM}}(b\bar{b} \to \Phi)\frac{\Gamma(\Phi\to b\bar{b})^{\text{MSSM}}}{\Gamma(\Phi\to b\bar{b})^{\text{SM}}}$, where $\sigma^{\text{SM}}(b\bar{b} \to \Phi)$ is the total SM cross-section for production of Higgs boson with mass m_Φ via $b\bar{b}$ fusion: to obtain the value in the MSSM it is rescaled with the ratio of the decay

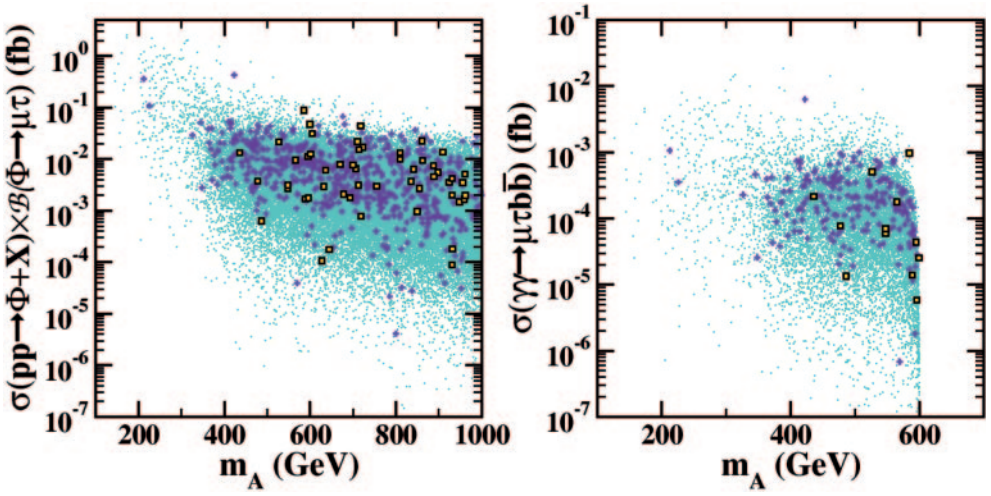

Fig. 1. – (Colour on-line) Left: scatter plot of the inclusive production cross-section $pp \to \Phi + X$ times the branching ratio of $\Phi \to \tau\mu$ at LHC *vs.* m_A ($\Phi = A, H$). Right: scatter plot for the cross-section of the process $\gamma\gamma \to \tau\mu b\bar{b}$ in photon-photon collision at $\sqrt{s_{\gamma\gamma}} = 600\,\text{GeV}$. The light gray (turquoise) points have only $\Omega_\chi h^2 \leq 0.13$ and $a_\mu^{\text{MSSM}} \leq 4 \times 10^{-9}$, the plus-shaped dark-gray (indigo) points satisfy $0.09 \leq \Omega_\chi h^2 \leq 0.13$ and $a_\mu^{\text{MSSM}} \leq 4 \times 10^{-9}$, finally, the squared points satisfy $0.09 \leq \Omega_\chi h^2 \leq 0.13$ and $1 \times 10^{-9} \leq a_\mu^{\text{MSSM}} \leq 4 \times 10^{-9}$.

width of the inverse process in the MSSM over the SM decay width [9]. We calculate for each random model the product $\sigma(pp \to \Phi + X) \times \mathcal{B}(\Phi \to \tau\mu)$. As masses and couplings of A and H are practically identical as discussed above, we have $\sigma(pp \to A+X)+\sigma(pp \to H + X) \simeq 2\sigma(pp \to A + X)$. The scatter plot $\sigma(pp \to \Phi + X) \times \mathcal{B}(\Phi \to \tau\mu)$ is shown in fig. 1, left panel. We see that with the nominal integrated luminosity of $100\,\text{fb}^{-1}$ per year models which satisfy both the relic density abundance and Δa_μ can give up to 10 events per year (squared points), up to 40 if we relax the condition on the lower limit of Δa_μ (plus-shaped points) and up to 200-300 relaxing both the lower limits (turquoise (light-gray) points).

In $\gamma\gamma$ collisions the main production mechanism for $\Phi = A, H$ is $\tau\tau$ fusion while the $b\bar{b}$ is suppressed by a factor $3(1/3)^4(m_b/m_\tau)^2 \simeq 0.1$ which cannot be compensated by corrections to the b Yukawa coupling. In ref. [11] we studied in detail the $\mu\tau$ fusion process $\gamma\gamma \to \mu\tau b\bar{b}$ where the Higgs boson is produced in the s-channel via a virtual $\mu\tau$ pair and can be detected from its decay mode $A \to b\bar{b}$. There we have shown that a good analytical approximation for the cross-section is obtained using the equivalent particle approximation wherein the colliding real photons split, respectively, into τ and μ pairs with the subsequent $\mu\tau$ fusion into the Higgs boson and that the effect of photons spectra can be neglected. We thus consider monochromatic photons with $\sqrt{s_{\gamma\gamma}} = 600\,\text{GeV}$, and photon-photon luminosity $500\,\text{fb}^{-1}\,\text{y}^{-1}$ [11]. The scatter plot of the signal cross-section *versus* m_A is shown in fig. 1, right panel. Here the models which satisfy both the relic density abundance and Δa_μ (squared points) have maximal cross-section $10^{-3}\,\text{fb}$, which is too small. Relaxing the lower limits cross-sections up to $2 \times 10^{-2}\,\text{fb}$ are possible, giving 10 events/year.

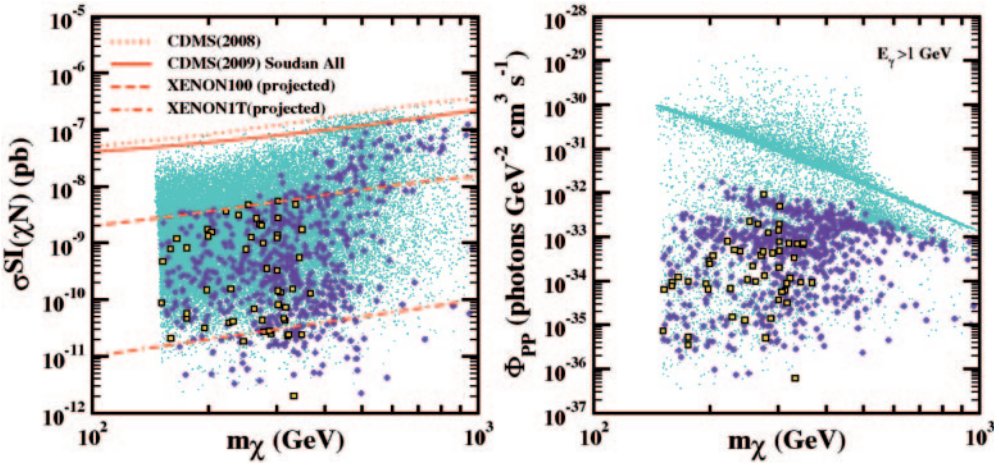

Fig. 2. – (Colour on-line) Left: scatter plot for the spin-independent neutralino-nucleon cross-section *vs.* the neutralino mass. The area above the solid line is excluded by the CDMS final results; the area above the dotted line is excluded by the 2008 CDMS search. The dashed and dot-dashed lines give the sensitivity reach of two phases of the XENON experiment. Right: scatter plot for the particle physics factor entering the formula of the flux of gamma-rays from neutralino annihilation in the halo, see the text. The light gray (turquoise) points have only $\Omega_\chi h^2 \leq 0.13$ and $a_\mu^{\mathrm{MSSM}} \leq 4 \times 10^{-9}$, the plus-shaped dark-gray (indigo) points satisfy $0.09 \leq \Omega_\chi h^2 \leq 0.13$ and $a_\mu^{\mathrm{MSSM}} \leq 4 \times 10^{-9}$, finally, the squared points satisfy $0.09 \leq \Omega_\chi h^2 \leq 0.13$ and $1 \times 10^{-9} \leq a_\mu^{\mathrm{MSSM}} \leq 4 \times 10^{-9}$.

3. – Neutralino dark matter direct and indirect detection

The spin-independent neutralino-nucleon cross-section in the limit of heavy squarks and large $\tan\beta$ can be approximated as [12] $\sigma^{\mathrm{SI}} \simeq \frac{g'^2 g^2 |N_{11}|^2 |N_{13}|^2 m_N^4}{4\pi m_W^2 m_A^4} \tan^2\beta \times K_f$, where N_{11} and N_{13} are the lightest neutralino unitary mixing matrix elements, m_N the nucleon mass (neglecting the mass difference between the neutron and the proton) and K_f a factor which depends on nucleon form factors. The left panel of fig. 2 shows the scatter plot for the spin-independent neutralino-nucleon cross-section as a function of m_χ and the region excluded by CDMS [5]. We emphasize that CDF and CDMS limits are very mild constraints: the region excluded by CDF is practically excluded by the other constraints while the CDMS limit excludes only one plus-shaped point leaving untouched the regions preferred by WMAP and the $(g-2)_\mu$ anomaly. The XENON100 experiment [13] should reach the sensitivity corresponding to the dashed gray (red) line in fig. 1, left panel. Such sensitivity is able to cover the region with the highest cross-section, $m_\chi \geq 300\,\mathrm{GeV}$, where there is a large higgsino component. On the other hand, the region preferred by $(g-2)_\mu$ anomaly cannot be covered. We also report the prospected sensitivity goal of the XENON experiment with 1 ton detector mass [13], dot-dashed gray (red) line, which is 10^{-11}–$10^{-10}\,\mathrm{pb}$ for neutralino mass in the range 100–1000 GeV: practically all of the parameter space can be probed.

We also present the effect of our constrained parameter space on the flux of photons coming from neutralino annihilation in the halo which is a very active field in indirect dark matter detection. The flux of gammas expected from neutralino annihilation is generally given by $F = \Phi_{PP} \times \Phi_{\mathrm{astro}}$ where the second factor contains the astrophysi-

cal information and is given by the integral of the squared of the dark matter density along the direction of observation, while Φ_{PP} is the particle physics factor given by $\Phi_{PP}(E_\gamma > E_{\rm th}) = \langle\sigma v\rangle/(2m_\chi^2)\int_{E_{\rm th}}^{m_\chi} {\rm d}E({\rm d}N_\gamma/{\rm d}E)$, where $\langle\sigma v\rangle$ is the thermal averaged cross-section annihilation times the velocity of neutralinos and the ${\rm d}N_\gamma/{\rm d}E$ is the photon spectrum which is integrated over energies greater than $E_{\rm th}$. Here we are interested mainly in the evaluation of the particle physics factor and in comparing it with other studies in the literature in the framework of the MSSM. We present Φ_{PP} as a function of the neutralino mass in fig. 2, right panel, with threshold energy $E_{\rm th} = 1\,{\rm GeV}$. For models with a relic density inside the WMAP interval the maximum value of the particle physics factor is 2×10^{-32} photons ${\rm GeV}^{-2}\,{\rm cm}^3\,{\rm s}^{-1}$ for neutralino mass around 200 GeV: this value is two orders of magnitude smaller than the typical values found in similar studies without the constraints from lepton flavor violation and the updated B physics and $(g-2)_\mu$ constraints, see refs. [14]. We remark that most of the models which satisfy the WMAP bounds, the plus-shaped and squared points in the figures, satisfy the Higgs funnel condition $m_A \simeq 2m_\chi$ (see fig. 2, left panel of ref. [10]): the main annihilation channel is $\chi\chi \to b\bar{b}/\tau\bar{\tau}$ through s-channel heavy Higgs exchange which is strongly constrained in our scenario and thus it is natural to have a reduction of photon emission. A reduction of the gamma-ray flux in the funnel region is also found in ref. [3] in the study of the minimal supergravity (mSUGRA) plus right-handed neutrinos for see-saw generation of neutrino masses respect to the case of pure mSUGRA.

4. – Conclusions

In the framework of the MSSM with heavy SUSY-QCD particles and large $\tan\beta$ we have studied lepton flavor violation in $\tau - \mu$ sector mediated by the heavy neutral Higgs $\Phi = A$, H at high-energy colliders through the production and decay at LHC, $pp \to \Phi + X$, $\Phi \to \tau\mu$ and the $\mu - \tau$ fusion at a photon collider, $\gamma\gamma \to \tau\mu b\bar{b}$.

We have found that in models with $0.09 \leq \Omega_\chi h^2 \leq 0.13$ and $1 \leq a_\mu^{\rm MSSM} \times 10^9 \leq 4$: at LHC the cross-section for $pp \to \Phi + X$, $\Phi \to \tau\mu$ can reach $\mathcal{O}(10^{-1}$–$10^{-2})\,{\rm fb}$ in the range $m_A = 400$–$1000\,{\rm GeV}$ giving up to 10 events with $100\,{\rm fb}^{-1}$; the cross-section of $\gamma\gamma \to \tau\mu b\bar{b}$ reaches $\mathcal{O}(10^{-3})\,{\rm fb}$, thus too small even for the large value of the expected luminosity of $500\,{\rm fb}^{-1}$. Prospects are somewhat more encouraging if we relax the lower limits, imposing only $\Omega_\chi h^2 \leq 0.13$ and $a_\mu^{\rm MSSM} \times 10^9 \leq 4$: the cross-section at LHC is about 2 fb for low m_A masses and around $2 \times 10^{-2}\,{\rm fb}$ in $\gamma\gamma$ collisions. On the other hand, to observe such effects, in any case, the full luminosity of the machine is needed.

We have also studied the spin-independent neutralino nucleus cross-section: we have shown that in models that satisfy $0.09 \leq \Omega_\chi h^2 \leq 0.13$ and $1 \leq a_\mu^{\rm MSSM} \times 10^9 \leq 4$, the cross-section lies just below the sensitivity of XENON100 which should report results soon. The full XENON 1 ton is needed to cover all the parameter space. For models with a relic density inside the WMAP interval the particle physics factor for gamma-rays flux from neuralino annihilation in the haloes is found to be smaller than the typical values found in similar studies without the constraints from lepton flavor violation and the updated B physics and $(g-2)_\mu$ constraints.

* * *

MC acknowledges support by the project P07FQM02962 funded by "Junta de Andalucia", partial support by the FPA2008-04073-E/INFN project and MULTIDARK project of Spanish Ministry of Science and Innovation's Consolider-Ingenio Ref: CSD2009-00064.

REFERENCES

[1] Djouadi A., *Phys. Rep.*, **459** (2008) 1 [arXiv:hep-ph/0503173].

[2] Jungman G., Kamionkowski M. and Griest K., *Phys. Rep.*, **267** (1996) 195 [arXiv:hep-ph/9506380]; Bertone G., Hooper D. and Silk J., *Phys. Rep.*, **405** (2005) 279 [arXiv:hep-ph/0404175].

[3] Barger V., Marfatia D. and Mustafayev A., *Phys. Lett. B*, **665** (2008) 242 [arXiv:0804.3601 [hep-ph]]; Barger V., Marfatia D., Mustafayev A. and Soleimani A., *Phys. Rev. D*, **80** (2009) 076004 [arXiv:0908.0941 [hep-ph]].

[4] Babu K. S. and Kolda C., *Phys. Rev. Lett.*, **89** (2002) 241802 [arXiv:hep-ph/0206310]; Sher M., *Phys. Rev. D*, **66** (2002) 057301 [arXiv:hep-ph/0207136]; Dedes A., Ellis J. R. and Raidal M., *Phys. Lett. B*, **549** (2002) 159 [arXiv:hep-ph/0209207]; Brignole A. and Rossi A., *Phys. Lett. B*, **566** (2003) 217 [arXiv:hep-ph/0304081]; *Nucl. Phys. B*, **701** (2004) 3 [arXiv:hep-ph/0404211]; Arganda E., Curiel A. M., Herrero M. J. and Temes D., *Phys. Rev. D*, **71** (2005) 035011 [arXiv:hep-ph/0407302]; Kanemura S., Ota T. and Tsumura K., *Phys. Rev. D*, **73** (2006) 016006 [arXiv:hep-ph/0505191]; Parry J. K., *Nucl. Phys. B*, **760** (2007) 38 [arXiv:hep-ph/0510305]; Paradisi P., *JHEP*, **02** (2006) 050 [arXiv:hep-ph/0508054]; Chen C. H. and Geng C. Q., *Phys. Rev. D*, **74** (2006) 035010 [arXiv:hep-ph/0605299]; Herrero M. J., Portoles J. and Rodriguez-Sanchez A. M., *Phys. Rev. D*, **80** (2009) 015023 [arXiv:0903.5151 [hep-ph]]; Diaz-Cruz J. L., Ghosh D. K. and Moretti S., *Phys. Lett. B*, **679** (2009) 376 [arXiv:0809.5158 [hep-ph]]; Kanemura S. and Tsumura K., *Phys. Lett. B*, **674** (2009) 295 [arXiv:0901.3159 [hep-ph]].

[5] Ahmed Z. *et al.* (CDMS Collaboration), *Phys. Rev. Lett.*, **102** (2009) 011301 [arXiv:0802.3530 [astro-ph]]; Ahmed Z. *et al.* (The CDMS-II Collaboration), [arXiv:0912.3592 [astro-ph.CO]].

[6] Aaltonen T. *et al.* (CDF Collaboration), [arXiv:0906.1014 [hep-ph]].

[7] Spergel D. N. *et al.* (WMAP Collaboration), *Astrophys. J. Suppl.*, **170** (2007) 377 [arXiv:astro-ph/0603449].

[8] Gondolo P., Edsjö J., Ullio P., Bergström L., Schelke M. and Baltz E. A., *JCAP*, **0407** (2004) 008 [arXiv:astro-ph/0406204].

[9] Heinemeyer S., Hollik W. and Weiglein G., *Comput. Phys. Commun.*, **124** (2000) 76 [arXiv:hep-ph/9812320].

[10] Cannoni M. and Panella O., *Phys. Rev. D*, **81** (2010) 036009 [arXiv:0910.3316 [hep-ph]].

[11] Cannoni M. and Panella O., *Phys. Rev. D*, **79** (2009) 056001 [arXiv:0812.2875 [hep-ph]]; *Nuovo Cimento C*, **32** (2009) 229 [arXiv:0910.2579 [hep-ph]]; Cannoni M., Carimalo C., Da Silva W. and Panella O., *Phys. Rev. D*, **72** (2005) 115004 [arXiv:hep-ph/0508256].

[12] Carena M. S., Hooper D. and Skands P. Z., *Phys. Rev. Lett.*, **97** (2006) 051801 [arXiv:hep-ph/0603180]; Carena M. S., Hooper D. and Vallinotto A., *Phys. Rev. D*, **75** (2007) 055010 [arXiv:hep-ph/0611065].

[13] Aprile E. and Baudis L. (Xenon100 Collaboration), *PoS*, **IDM2008** (2008) 018 [arXiv:0902.4253 [astro-ph.IM]].

[14] Fornengo N., Pieri L. and Scopel S., *Phys. Rev. D*, **70** (2004) 103529 [arXiv:hep-ph/0407342]; Sanchez-Conde M. A., Prada F., Lokas E. L., Gomez M. E., Wojtak R. and Moles M., *Phys. Rev. D*, **76** (2007) 123509 [arXiv:astro-ph/0701426].